

Detection of OH 18-cm Emission from Comet C/2020 F3 NEOWISE using the Arecibo Telescope

ALLISON J. SMITH,^{1,2} D. ANISH ROSHI,^{1,2} PERIASAMY MANOHARAN,^{1,2} SRAVANI VADDI,^{1,2} BENETGE B. P. PERERA,^{1,2} AND ANNA MCGILVRAY^{1,2}

¹*Arecibo Observatory, Arecibo, PR, 00612, USA*

²*University of Central Florida, Orlando, FL, 32816, USA*

ABSTRACT

We report the detection of emission from the OH 18 cm Λ -doublet transitions toward Comet C/2020 F3 NEOWISE using the Arecibo Telescope. The antenna temperatures are 113 ± 3 mK for the 1667 MHz line and 57 ± 3 mK for the 1665 MHz line. The beam averaged OH column density (centered on the comet nucleus) derived from the 1667 transition is $N_{OH} = 1.11 \pm 0.06 \times 10^{13}$ cm⁻². We implemented the Haser model to derive an OH production rate. The estimated OH production rate using the 1667 transition is $Q_{OH} = 3.6 \pm 0.6 \times 10^{28}$ s⁻¹, a factor of 2.4 lower than optically derived values for the same observing day, the difference of which is likely explained by quenching.

Keywords: Long period comets (933), Comets (280), Molecular spectroscopy (2095), Radio spectroscopy (1359)

1. INTRODUCTION

Discovered by astronomers associated with the *NEOWISE* mission of the Wide-field Infrared Survey Explorer spacecraft (Mainzer et al. 2011) on March 27, 2020, Comet C/2020 F3 (NEOWISE)¹ produced a vibrant show in the northern hemisphere during the summer of 2020, exciting both casual observers and astronomers alike. The comet reached perihelion on July 3, 2020 at a heliocentric distance of 0.3 AU, and continued on a trajectory that was favorable for Earth-based observations, presenting a unique opportunity to observe its composition and behavior (see Knight & Battams 2020; Manzini et al. 2020; Lin et al. 2020; Krishnakumar et al. 2020; Drahus et al. 2020; Smith et al. 2020, for some early reports).

As comets spend most of their existence preserved in the icy outer Solar System, investigation of their astrochemistry is paramount for understanding the conditions when the Solar System was forming (A'Hearn 2017, and references therein). Observations reveal a slew of molecules, likely released when the rapid temperature change incurred by the comet's approach toward the Sun causes water-ice to sublime from the sub-surface nucleus into the coma (Despois et al. 2005). That the molecular abundances vary for individual comets under-

scores the importance of gathering data on their chemistry when opportunities arise.

The hydroxyl (OH) molecule is the most common volatile and is generally used to assess the production of water as well as serving as a standard by which to compare other molecular abundances in cometary comae (Feldman 2006). Biraud et al. (1974) first reported the detection of the 18 cm lines in comets. While electronic and vibrational transitions of OH are observable in the UV and infrared, the spectral resolution provided by radio observations of the hyperfine Λ -doublet transitions at 18-cm wavelength provides unique information on the velocity, distribution, and turbulence characteristics of the outflowing gas (Crovisier et al. 2016). The levels of the transition may be inverted or anti-inverted through UV pumping and fluorescence (Biraud et al. 1974; Mies 1974; Despois et al. 1981; Schloerb 1988) and be manifest in observations as emission or absorption lines accordingly. Observing the Λ -doublet in cometary atmospheres often requires accounting for quenching of the inversion by collisions with electrons and ions, a phenomenon that has long been the subject of theoretical and observational investigations, and the neglect of which may result in underestimation of the OH production rate (Crovisier et al. 2002, and references therein).

The structure of this paper is as follows. We describe in § 2 our observational setup and outline the steps taken to reduce the data in § 3. We discuss the results in § 4

¹ The Minor Planet Electronic Circular 2020-G05 is available at <https://minorplanetcenter.net/mpec/K20/K20G05.html>.

Table 1. Orbital Parameters of Comet NEOWISE.

Parameter ^a	Value
UT range	July 31.781–July 31.875
Heliocentric distance (r_h)	0.82 AU
Geocentric distance	0.79 AU
Heliocentric velocity (V_h)	37.17 km s ⁻¹
Geocentric velocity	34.92 km s ⁻¹
Sun-target-observer (STO) angle	78°

^aTables values (aside from UT range) are quoted for the middle of the observing run.

and the implications in § 5. Finally we conclude with a summary in § 6.

2. OBSERVATIONS

We observed Comet NEOWISE on July 31, 2020, using the 305-m radio telescope at the Arecibo Observatory (AO) in Puerto Rico, USA, during Director’s Discretionary Time (Project A3470). We obtained the orbital parameters of the comet from the JPL HORIZONS system² (Giorgini et al. 1996) and present these in Table 1. We used the L-band Wide (LBW) receiver and configured the Wideband Arecibo Pulsar Processors (WAPPs) to observe simultaneously the OH main and satellite lines at 1665, 1667, 1612, and 1720 MHz. The total bandwidth for each subcorrelator board was 1.5625 MHz, each subdivided into 2048 channels, resulting in a spectral resolution of 0.7 kHz, i.e., 0.1 km s⁻¹. As the LBW spectral baselines are stable on frequency scales comparable to the expected OH linewidths of the comet, we used the ON-only mode for our observations. The beam efficiency, η_{MB} , near 1667 MHz is $\sim 60\%$ and the half power beam width, $\theta_B \sim 2.9'$. The mean zenith angle of the observations was 15°. We observed a single pointing centered on the nucleus for the duration of the observations, approximately 110 min (consisting of 22×5 min scans), and did not apply an on-line Doppler correction.

3. DATA PROCESSING

We processed these data using both existing³ and new routines developed with the Interactive Data Language (IDL) package. We first performed a quality check of the data by visual inspection of all 22 scans, each of

which consists of 300 one-second integrations, and then averaged the two orthogonal linear polarization channels. There was no noticeable Radio Frequency Interference in our data. The antenna temperatures quoted are obtained using a calibrated noise source for which the average noise temperatures of the diodes were 8.48 and 9.35 K respectively, for the two polarizations. The shape of the bandpass was corrected for the calibrated spectrum by fitting a 3rd or 4th order polynomial to the line free channels and first subtracting and then dividing the spectrum by the polynomial. We then multiplied by the system temperature to retain the amplitude calibration. We obtained the final spectra by averaging the reduced data from all 22 scans and applying a velocity correction to account for the earth’s rotation (217 m s⁻¹). The source velocity changed by 245 m s⁻¹ during the observations, and we used an FFT interpolation method to re-sample each calibrated spectrum during the averaging process in order to apply this correction.

4. RESULTS

These observations consist of a single observing session on Comet NEOWISE. While subsequent observations were planned, they were interrupted by the temporary shutdown of the Arecibo telescope due to the failure of one of its auxiliary cables supporting the telescope feed platform on August 10, 2020. Nevertheless, we detected relatively strong emission from the OH 18-cm main lines at 1665 and 1667 MHz during the first and only session. The line antenna temperature, T_A , spectral RMS, full-width at half maximum line width, ΔV , and line central velocity with respect to the comet reference frame, V_{CF} , obtained with a single-Gaussian model (see Fig. 1) are given in Table 2. The observed central velocities of the line are close to the expected line-of-sight velocity (34.92 km s⁻¹) and are thus likely associated with the comet. We also used SIMBAD⁴ (Wenger et al. 2000) to confirm that there are no background OH sources (e.g., a molecular cloud) likely to produce a signal that could be confused with the signal from the comet.

The detected line strengths in our observations are within the range of line amplitudes previously detected toward comets in Arecibo observations (Lovell et al. 2002) sampling similar physical scales at the source and heliocentric distances. The linewidths are also comparable, and the 1667:1665 line amplitude ratio is 1.98 ± 0.12 , marginally higher than the Local Thermodynamic Equilibrium (LTE) value of 1.8. This implies the 1667 MHz line was likely crossing the transition from absorption to

² <https://ssd.jpl.nasa.gov/horizons.cgi>

³ <http://www.naic.edu/~phil/software/software.html#idldoc>

⁴ <http://simbad.u-strasbg.fr/simbad/>

Table 2. Parameters of the OH 18-cm lines

Rest Freq.	T_A	RMS ^a	ΔV	V_{CF}	$\int T_L dV$
(MHz)	(mK)	(mK)	(km/s)	(km/s)	(mK km/s)
1612.2310	9(3)	8.3	1.8(0.7)	-0.16(0.30)	17(9)
1665.4018	57(3)	7.6	2.3(0.1)	0.08(0.05)	139(10)
1667.3590	113(3)	7.8	2.5(0.1)	0.06(0.03)	301(15)
1720.5300	10(4)	11.6	2.7(1.1)	-1.24(0.48)	29(18)

^aCorresponds to a velocity resolution of 0.14 km s⁻¹.

emission slightly ahead of the 1665 MHz line (see [Elitzur 1981](#)). The averaged spectra for all four lines are shown in Fig. 1. Low-amplitude signals are visible at the expected velocity and LTE intensity for the satellite lines, though the peak amplitudes are only at the 1- σ level.

5. DISCUSSION

5.1. Haser Model and OH Production Rate

Observations of the Λ -doublet yield useful information on the total production rate of OH (Q_{OH}), the calculation of which requires knowledge of the OH distribution and excitation state. In order to estimate Q_{OH} , we implement the Haser Model, which assumes a spherical coma with the Haser density distribution for the daughter molecule (in our case, OH). We cross-check our results with the vectorial model ([Combi & Delsemme 1980](#)) to assess their robustness and present alongside each other the parameters from both models following our description of the Haser calculation (see Table 3).

The Haser density distribution depends on Q_{OH} , the daughter scale length (l_d), and the parent scale length (l_p), and requires a constant radial velocity for the daughter molecule ($v_d = |\vec{v}_d|$). Following [Despois et al. \(1981\)](#), we consider l_p and l_d scale with heliocentric distance as r_h^2 . Q_{OH} is a variable, which is determined by matching the model integrated line flux density with the observed value.

To compute the line amplitude, we consider a coordinate system ($x'-y'-z'$ in Fig. 2) placed at the center of the comet nucleus in which the x' coordinate points towards Earth. We use a second coordinate system ($x-y-z$ in Fig. 2) to compute the heliocentric velocities of the particles. The x -axis of this coordinate system points towards the Sun. The two coordinate systems are rotated about the z -axis and the angles $x-O-x'$ is the Sun-target-observer (STO) angle. The space from 0 to $10 \times l_d$ is divided into N_{grid} logarithmic intervals along x' , y' & z' coordinates. The density at the center of each cell in space is obtained from the Haser distribution, and

the excitation state of OH is specified through the inversion parameter i (see [Schleicher & A'Hearn 1988](#)). It is well established that the excitation state oscillates between inverted (i is positive) and anti-inverted (i is negative) states with heliocentric velocity ([Crovisier et al. 2002](#)). Since the heliocentric velocity of the daughter molecule is the vector sum of the heliocentric velocity of the comet \vec{V}_h and \vec{v}_d , we calculate it by summing up the x -component of \vec{v}_d at the center of a given cell with $V_h = |\vec{V}_h|$. This velocity is then used to assign an inversion value to each cell.

Based on the basic assumption of the Haser model, the line emission from each cell when observed from Earth will fall in the interval $-v_d$ to v_d . Therefore, to obtain the line temperature as a function of velocity (i.e., to get the line profile), we divide the expected velocity interval (i.e., $2 v_d$) into N_v bins. Thus the velocity resolution in the simulation is $\Delta v = \frac{2v_d}{N_v}$ and the corresponding frequency resolution is $\Delta\nu$. The observed velocity of emission from a cell would be the projection of \vec{v}_d at the cell center in the direction of Earth. The line brightness temperature from a cell $T_L(v)$ in K for the optically thin case is (see Eq 6 of [Schloerb & Gerard 1985](#))

$$T_L(v) = C (T_{bg} + T_{L,bg}(v)) n_d i \Delta x' \frac{1}{\Delta\nu}, \quad (1)$$

where $C = 6.253 \times 10^{-10}$ cm² s⁻¹ for the 1667 transition, T_{bg} is the background continuum temperature in K, $T_{L,bg}(v)$ is the contribution to the background temperature in K due to line emission from all the cells behind the cell under consideration at the velocity v , n_d is the daughter density at the cell center in cm⁻³, and $\Delta x'$ is the line-of-sight thickness of the cell in cm. Assuming the line emission in a velocity bin is uniform, the line profile function is $\phi(v) = \frac{1}{\Delta\nu}$ and has units 1/Hz. The line brightness temperature vs. velocity in a grid parallel to the $y'-z'$ plane is obtained by summing the contributions from all the cells along the line of sight. The antenna temperature is then obtained by the weighted sum of the brightness temperature (see Eq. 12 of [Schloerb & Gerard 1985](#)); the weights are determined by the FWHM observing beam, beam efficiency and the geocentric distance to the comet. The integrated line antenna temperature in units of K km s⁻¹ is the sum of the antenna temperature over the velocity bins multiplied by Δv .

It is now established that when using the Haser model to estimate the production rate, equivalent values for the radial velocity and scale lengths need to be used (see [Combi & Delsemme 1980](#)). The production rate estimated with 'Haser equivalent' parameters compares well with predictions from, for example, the vectorial model (see [Bockelée-Morvan et al. 1990](#)). In our model,

we used $l_{pH} = 2.4 \times 10^4$ km and $l_{dH} = 1.6 \times 10^5$ km (A’Hearn et al. 1995), where l_{dH} and l_{pH} are used to denote that they are equivalent values at 1AU, and scaled them by r_h^2 to get l_p and l_d for the computation. These values are the same scale lengths used for the estimation of the production rate from optical OH observations of Comet NEOWISE (Schleicher, D. private communication). We assumed that the OH ejection velocity is 1.0 km s^{-1} (Bockelée-Morvan et al. 1990). Using the trapezium line profile modeling method (Bockelée-Morvan et al. 1990), we estimated the parent velocity as $1.12 \pm 0.05 \text{ km s}^{-1}$. The Haser equivalent daughter velocity is then $v_{dH} = 1.49 \text{ km s}^{-1}$ (see Combi & Delsemme 1980), which is used in the model to get the density distribution. We found that only the Schleicher & A’Hearn (1988) inversion curve predicts an emission line at the heliocentric velocity of the observed comet. Therefore in our model we used their inversion values (Table 5 of Schleicher & A’Hearn 1988).

We used $N_v = 9$ and $N_{grid} = 200$ for the results presented in this paper. We found that the results are not affected by the grid size if $N_{grid} \geq 200$. We also compared the model predictions with computations made using a linear sampling of space and the results were found to be consistent with the logarithmic sampling.

The OH production rate obtained with our Haser model for Comet NEOWISE is $3.6 \pm 0.6 \times 10^{28} \text{ s}^{-1}$ (see Table 3). In Fig. 2, the production rate obtained for Comet NEOWISE is compared with rates obtained for other comets (data taken from Schloerb et al. 1987; Tacconi-Garman et al. 1990). The integrated line intensity of the 1667 MHz transition was used for the estimation. The values for heliocentric velocity, geocentric distance and STO used for this computation are listed in Table 1. The T_{bg} towards the observed position is estimated as follows. The Galactic background temperature was obtained from the 408 MHz all-sky radio continuum survey (Haslam et al. 1982) and the value after removing the Cosmic Microwave Background (CMB) contribution is scaled to 1667 MHz using a spectral index of -2.6 . The estimated T_{bg} , including contribution from the CMB, is 3.23 ± 0.05 K. The N_{OH} , which represents the average over the Arecibo beam (centered on the comet nucleus), is estimated from the 1667 MHz transition to be $1.11 \pm 0.06 \times 10^{13} \text{ cm}^{-2}$.

We obtained an independent Q_{OH} estimate of $4.4 \pm 0.07 \times 10^{28} \text{ s}^{-1}$ from vectorial model calculations via Amy Lovell (Agnes Scott College, private communication). The vectorial Q_{OH} and our Q_{OH} are within the respective uncertainties of each model, and our Q_{OH} is 82% of the vectorial value (see Table 3 for a comparison). The production rate estimated from optical OH line ob-

servations for the same observation date is $8.5 \times 10^{28} \text{ s}^{-1}$ (Schleicher, D. private communication). We suggest that the difference between these two estimates could be due to the effects of quenching.

Table 3. Summary of Model Results

Input parameter values	Q_{OH} $\times 10^{28} \text{ s}^{-1}$	Note
$l_{dH} = 1.6 \times 10^5$ km, $l_{pH} = 2.4 \times 10^4$ km, $v_p = 1.12 \text{ km s}^{-1}$ $v_d = 1.0 \text{ km s}^{-1}$	3.6 ± 0.6	Haser equivalent model
$\tau_p = 8.2 \times 10^3$ s, $\tau_d = 1.5 \times 10^5$ s, $v_d = 1.0 \text{ km s}^{-1}$	4.4 ± 0.7	Vectorial model
$l_{dH} = 1.6 \times 10^5$ km, $l_{pH} = 2.4 \times 10^4$ km	8.5	Optical obs.
Note – l_{dH} , l_{pH} , the parent lifetime τ_p , the daughter lifetime τ_d are values at 1AU. The v_p obtained from vectorial model is $1.22 \pm 0.07 \text{ km s}^{-1}$		

6. SUMMARY

We have observed emission lines from the OH 18-cm Λ -doublet transitions in Comet NEOWISE. We implemented a Haser model to derive the Q_{OH} . For the Haser equivalent model parameters, we got $Q_{OH} = 3.6 \pm 0.6 \times 10^{28} \text{ s}^{-1}$, which compares well with the values obtained with the vectorial model. The estimated OH column density $N_{OH} = 1.11 \pm 0.06 \times 10^{13} \text{ cm}^{-2}$. The derived Q_{OH} is a factor of 2.4 lower compared to the optically derived value ($8.5 \times 10^{28} \text{ cm}^{-2}$), which is likely due to quenching.

7. ACKNOWLEDGEMENTS

We are grateful for the Director’s Discretionary Time dedicated to this project and for the assistance of Phil Perillat (AO) for his help with ephemeris tracking and telescope adjustments during the observations that led to high quality data. Amy Lovell gave extremely helpful input and provided an independent verification of the production rate using her vectorial modeling software. We very much appreciate valuable discussions with Dave Schleicher as well as the optical parameters he contributed. Chris Salter, Tapasi Ghosh, Yan Fernandez, Noemí Pinilla-Alonso, and an anonymous referee all gave very useful feedback on the manuscript. We made

use of the SIMBAD database, operated at CDS, Strasbourg, France. The Arecibo Observatory is a facility of the NSF operated under cooperative agreement (#AST-

1744119) by the University of Central Florida (UCF) in alliance with Universidad Ana G. Méndez (UAGM) and Yang Enterprises (YEI), Inc.

REFERENCES

- A'Hearn, M. F. 2017, *Philosophical Transactions of the Royal Society of London Series A*, 375, 20160261, doi: [10.1098/rsta.2016.0261](https://doi.org/10.1098/rsta.2016.0261)
- A'Hearn, M. F., Millis, R. C., Schleicher, D. O., Osip, D. J., & Birch, P. V. 1995, *Icarus*, 118, 223, doi: [10.1006/icar.1995.1190](https://doi.org/10.1006/icar.1995.1190)
- Biraud, F., Bourgois, G., Crovisier, J., et al. 1974, *A&A*, 34, 163
- Bockelée-Morvan, D., Crovisier, J., & Gérard, E. 1990, *A&A*, 238, 382
- Combi, M. R., & Delsemme, A. H. 1980, *ApJ*, 237, 641, doi: [10.1086/157910](https://doi.org/10.1086/157910)
- Crovisier, J., Bockelée-Morvan, D., Colom, P., & Biver, N. 2016, *Comptes Rendus Physique*, 17, 985, doi: <https://doi.org/10.1016/j.crhy.2016.07.020>
- Crovisier, J., Colom, P., Gérard, É., et al. 2002, in *ESA Special Publication, Vol. 500, Asteroids, Comets, and Meteors: ACM 2002*, ed. B. Warmbein, 685–688
- Despois, D., Biver, N., Bockelée-Morvan, D., & Crovisier, J. 2005, in *IAU Symposium, Vol. 231, Astrochemistry: Recent Successes and Current Challenges*, ed. D. C. Lis, G. A. Blake, & E. Herbst, 469–478, doi: [10.1017/S1743921306007484](https://doi.org/10.1017/S1743921306007484)
- Despois, D., Gerard, E., Crovisier, J., & Kazes, I. 1981, *A&A*, 99, 320
- Drahus, M., Guzik, P., Stephens, A., et al. 2020, *The Astronomer's Telegram*, 13945, 1
- Elitzur, M. 1981, *ApJ*, 246, 354, doi: [10.1086/158929](https://doi.org/10.1086/158929)
- Feldman, P. D. 2006, in *NASA LAW 2006*, ed. P. F. Weck, V. H. S. Kwong, & F. Salama, 62
- Giorgini, J. D., Yeomans, D. K., Chamberlin, A. B., et al. 1996, in *AAS/Division for Planetary Sciences Meeting Abstracts #28, AAS/Division for Planetary Sciences Meeting Abstracts*, 25.04
- Haslam, C. G. T., Salter, C. J., Stoffel, H., & Wilson, W. E. 1982, *A&AS*, 47, 1
- Knight, M., & Battams, K. 2020, *The Astronomer's Telegram*, 13853, 1
- Krishnakumar, A., Angchuk, D., Venkataramani, K., et al. 2020, *The Astronomer's Telegram*, 13897, 1
- Lin, Z.-Y., Wang, C., Ip, W.-H., et al. 2020, *The Astronomer's Telegram*, 13886, 1
- Lovell, A. J., Howell, E. S., Schloerb, F. P., Lewis, B. M., & Hine, A. A. 2002, in *ESA Special Publication, Vol. 500, Asteroids, Comets, and Meteors: ACM 2002*, ed. B. Warmbein, 681–684
- Mainzer, A., Bauer, J., Grav, T., et al. 2011, *ApJ*, 731, 53, doi: [10.1088/0004-637X/731/1/53](https://doi.org/10.1088/0004-637X/731/1/53)
- Manzini, F., Ochner, P., Oldani, V., & Bedin, L. R. 2020, *The Astronomer's Telegram*, 13884, 1
- Mies, F. H. 1974, *ApJL*, 191, L145, doi: [10.1086/181572](https://doi.org/10.1086/181572)
- Schleicher, D. G., & A'Hearn, M. F. 1988, *ApJ*, 331, 1058, doi: [10.1086/166622](https://doi.org/10.1086/166622)
- Schloerb, F. P. 1988, *ApJ*, 332, 524, doi: [10.1086/166674](https://doi.org/10.1086/166674)
- Schloerb, F. P., Claussen, M. J., & Tacconi-Garman, L. 1987, *A&A*, 187, 469
- Schloerb, F. P., & Gerard, E. 1985, *AJ*, 90, 1117, doi: [10.1086/113819](https://doi.org/10.1086/113819)
- Smith, A., Manoharan, P., McGilvray, A., et al. 2020, *The Astronomer's Telegram*, 13968, 1
- Tacconi-Garman, L. E., Schloerb, F. P., & Claussen, M. J. 1990, *ApJ*, 364, 672, doi: [10.1086/169450](https://doi.org/10.1086/169450)
- Wenger, M., Ochsenbein, F., Egret, D., et al. 2000, *A&AS*, 143, 9, doi: [10.1051/aas:2000332](https://doi.org/10.1051/aas:2000332)

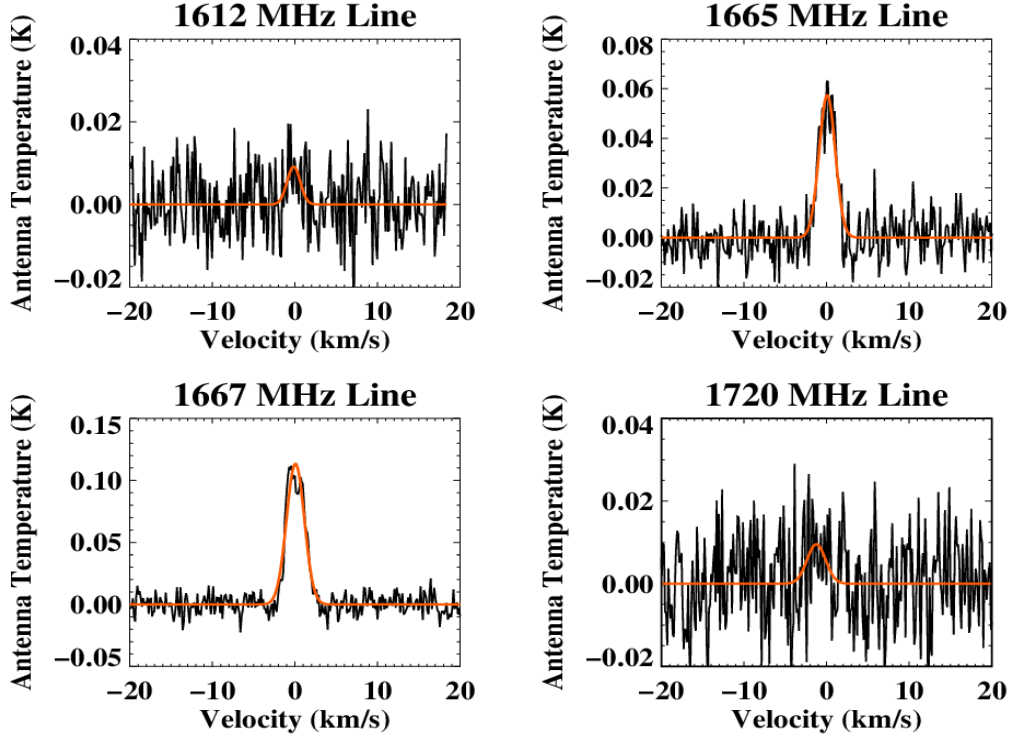


Figure 1. Final averaged spectra for all four OH 18-cm lines in the nucleus-centered frame along with a fitted single-component Gaussian model (orange).

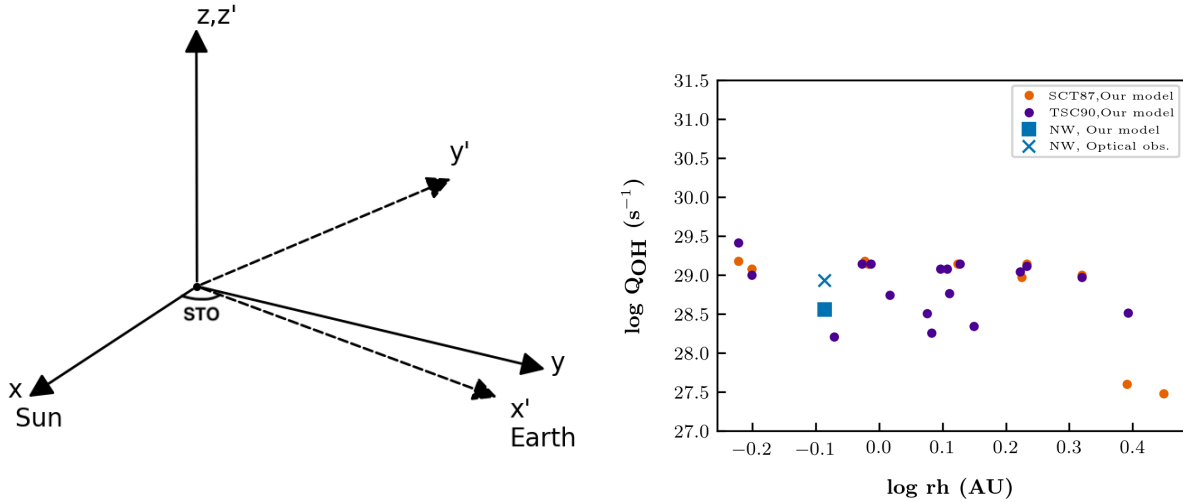


Figure 2. Left: The coordinate systems centered at the comet nucleus used in our model. The x' axis points toward Earth, while the x axis points toward the Sun. The two coordinates are rotated about the z -axis. The angle x - O - x' is the Sun-target-observer (STO) angle. Right: Comparison of Q_{OH} estimated for Comet NEOWISE with those obtained for other comets from literature. The Q_{OH} values estimated using our model for the comet data from Schloerb et al. (1987) and Tacconi-Garman et al. (1990) are marked using filled circles. These values are within a factor of 2 of Q_{OH} estimates given in Schloerb et al. (1987) and Tacconi-Garman et al. (1990). The Q_{OH} obtained for Comet NEOWISE is shown with filled square. The vertical width of the square is equal to the estimation error in Q_{OH} . For comparison, we also show the Q_{OH} estimated for Comet NEOWISE from the optical observations (shown with blue cross). The x -axis is the heliocentric distance in AU.